Conformational Flexibility of Domain III of Annexin V Studied by Fluorescence of Tryptophan 187 and Circular Dichroism: The Effect of PH†

Jana Sopkova,‡ Michel Vincent,‡ Masayuchi Takahashi,§ Anita Lewit-Bentley,‡ and Jacques Gallay*,‡

L.U.R.E. Laboratoire pour l'Utilization du Rayonnement Electromagnétique, Université Paris-Sud, Bâtiment 209D, B. P. 34, F-91898 Orsay Cedex, France, and UMR216, Institut Curie, Bâtiment 110, F-91405 Orsay Cedex, France

Received April 6, 1998; Revised Manuscript Received May 29, 1998

ABSTRACT: The conformation and dynamics of domain III of annexin V was studied by steady-state and time-resolved fluorescence of its single tryptophan residue (Trp187) as a function of pH in the absence of calcium. At neutral pH, the maximum of emission occurs at 326 nm, in agreement with the hydrophobic location of the tryptophan residue seen in the three-dimensional structure. Upon decreasing the pH, a progressive red-shift by about 12 nm of the fluorescence emission spectrum is observed. The effect is complete between pH 6 and 4.5, and most likely involves at least one and maybe two carboxylic group(s). Circular dichroism mesurements give evidence for a preservation of the native folding of the protein in these mild acidic conditions. A fluorescence red-shift of smaller amplitude is also observed at high pH (∼11). The aggregation state of the protein is affected by pH: while at neutral pH, the protein is monomeric (rotational correlation time = 14 ns); it forms aggregates larger than a dimer (rotational correlation time > 40 ns) in acidic pH conditions. These results suggest that electrostatic interactions are probably important for the stabilization of the folding of domain III without calcium. The conformational change may be related to the aggregation state of the molecule. Examination of the protein crystal structures with and without calcium ion in domain III shows an interplay of salt bridges implying charged amino acid side chains at the molecule surface of domain III. These observations may provide a further clue to the mechanism of the conformational change of domain III of annexin V induced by high calcium concentrations and interaction at the membrane/water interface.

Annexin V belongs to a family of water-soluble proteins which undergo reversible Ca^{2+}-dependent binding to phospholipid bilayers and specific cellular membranes *(1−3)*. Annexins are widely distributed in different species, tissues, and cell types. They are abundant in most eukaryotic cells, comprising up to 1% of the total cell proteins. It is therefore likely that they serve one or more important physiological functions, related most probably to their ability to bind to acidic phospholipid bilayers in a Ca^{2+}-dependent manner. Although these physiological functions are as yet unknown, the wide range of in vitro properties of these proteins has led to an even wider range of proposed in vivo functions. Some annexins appear to be involved in various types of membrane fusion events such as endo- and exocytosis, others exhibit anti-inflammatory and anti-coagulatory properties in vitro *(1)*. Some of these proteins display ion channel activity in vitro *(2)*. All annexins share a high sequence homology (∼ 40−60%) and contain a highly conserved core of a four- or 8-fold repeat of 70 residues, and a more variable N-terminal segment.

All crystal structures of annexins solved to date show that these sequence domains correspond to structural domains, each consisting of five α-helices (A to E) (for instance annexin V, ref *4*). Each structural domain contains generally one principal calcium binding site. The calcium ion is bound to carbonyl oxygens of the loop connecting helices A and B, and to a carboxyl of the negatively charged amino acid side chain (Glu or Asp) about 40 residues downstream, in the loop connecting helices D and E in the same domain. In annexin V, a particular situation prevails since the existence of the calcium binding site in domain III requires a large conformational change to take place. This change was observed by X-ray diffraction studies *(5−7)*, showing that the IIIA-IIIB loop is brought from a buried position onto the surface of the protein. At the same time, the position of the loop IIID-IIIE changes significantly, allowing glutamic acid 228 to approach the calcium site and to complete the calcium ligands (Figure 1).

The presence of the unique tryptophan residue (Trp187)[1] in the IIIA-IIIB loop has allowed us to study this conformational change by fluorescence spectroscopy *(8−11)*. These studies have shown that the conformational change was provoked by high concentrations (>millimolar) of calcium, in the absence of membranes. Trp187 becomes totally exposed to the solvent at the surface of the protein as suggested by the large red-shift of its fluorescence

† Partial financial supports from CNRS, CEA, MESRT, and EC are acknowledged. J.S. is a recipient of a postdoctoral grant from the EC (ERBBIO4CT960083).

* Author to whom correspondence should be addressed at L.U.R.E., Bâtiment 209D Université Paris-Sud, B. P. 34, 91898 Orsay, France. Telephone/Fax: 33 01 64 46 80 82. E-mail: gallay@lure.u-psud.fr.

‡ L.U.R.E. Laboratoire pour l'Utilisation du Rayonnement Electromagnétique.

§ Institut Curie.

[1] Abbreviations: Trp, tryptophan; MEM, maximum entropy method.

S0006-2960(98)00773-9 CCC: $15.00
Published on Web 08/07/1998

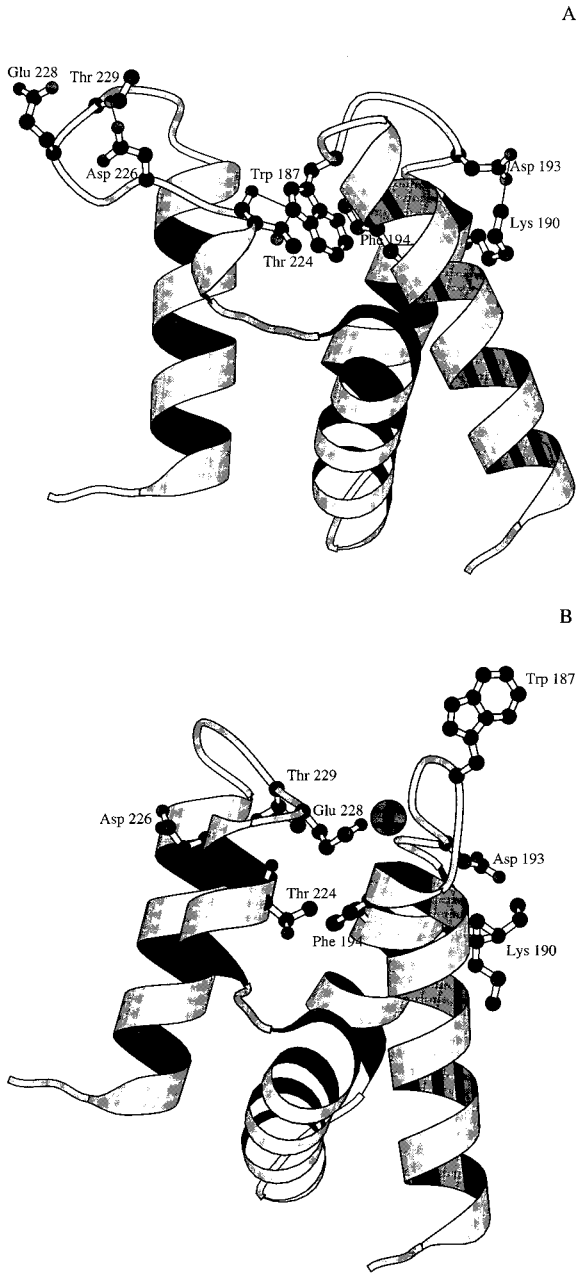

FIGURE 1: Ribbon representation of the three-dimensional structure of domain III in annexin V. (A) without calcium; (B) with the bound calcium ion (represented as a ball). Amino acid side chains of Trp187, Asp190, Lys193, Phe194, Thr224, Asp226, Glu228, and Thr229 are represented as balls-and-sticks. (Figures produced using Molscript) *(60)*.

maximum (~25 nm), in full agreement with the crystal structure *(5−7)*. A similar red-shift of the fluorescence emission spectrum has also been observed upon binding of the protein to negatively charged phospholipidic membranes but in the presence of lower concentrations of calcium *(8, 10−13)*. This suggests that this conformational change is similar to the one produced by higher concentrations of calcium in the absence of membranes. The significant difference in the calcium concentration dependence of the two processes has been attributed to a local concentration effect at the membrane surface *(14)* since negatively charged phospholipids can bind calcium in the millimolar concentration range *(15−18)*.

The mechanism of this conformational change remains nevertheless unclear, since calcium itself is needed to shape its own binding site. This occurs at a high concentration of the ion, suggesting that high calcium concentration is needed to disrupt stabilizing forces, such as salt bridges that could be present or not, depending on the presence of calcium in domain III. In this hypothesis, the ionization state of specific amino acid side chains can play a role in the conformational stability of domain III. It has recently been shown moreover, that the interaction of annexin V with phospholipid membranes was quite different at neutral and at mild acidic pH *(19)*. This could be related either to the change in the increase of the average hydrophobicity of the protein at pH 4 and/or to local conformational effects that have not yet been studied. We have therefore decided to monitor the possible changes in the environment of Trp187 and of the aggregation state of the protein as a function of pH, by means of steady-state and time-resolved fluorescence intensity and anisotropy decay measurements.

MATERIALS AND METHODS

Protein Preparation. Recombinant human annexin V was prepared as before *(20)*. In this procedure, calcium is removed during the purification by EDTA and the protein is stored in the absence of calcium. For measurements of absorbance, circular dichroism, and fluorescence, the protein solutions were prepared in the following buffers at 50 mM concentration: sodium acetate from pH 3.5 to 6, sodium cacodylate from pH 5 to 7, Tris-HCl from pH 7 to 9, and glycine-NaOH from pH 9 to 11. All chemicals were of analytical grade purity, obtained from Merck, France.

Steady-State Fluorescence Measurements. Tryptophan fluorescence emission spectra were recorded between 300 and 420 nm (bandwidth 4 nm) on a SLM 8000 spectrofluorometer equipped with Hamamatsu Photon Counting Detectors (model H3460-53) at an excitation wavelength of 295 nm (bandwidth 2 nm) using 5 × 5 mm or 10 × 10 mm optical path cuvettes. Blanks were always subtracted in the same experimental conditions. The protein concentration was 10 μM. To remove polarization artifacts, the fluorescence emission spectra were reconstructed from the four polarized spectra according to

$$I(\lambda) = I_{vv}(\lambda) + 2 \times G(\lambda) \times I_{vh}(\lambda)$$

where $G(\lambda)$ is a correction factor defined as

$$G(\lambda) = \frac{I_{hv}(\lambda)}{I_{hh}(\lambda)}$$

and $I_{vv}(\lambda)$, $I_{vh}(\lambda)$, $I_{hv}(\lambda)$, and $I_{hh}(\lambda)$ are the polarized fluorescence intensities at the emission wavelength λ after corresponding blank subtraction. The first and second subscripts refer to the orientation of the excitation and emission polarizers, respectively.

Time-Resolved Fluorescence Measurements. Fluorescence intensity and anisotropy decays were obtained by the time-correlated single photon counting technique from the $I_{vv}(t)$ and $I_{vh}(t)$ components recorded on the experimental setup installed on the SB1 window of the synchrotron radiation source Super-ACO (Anneau de Collision d'Orsay), which has been described before *(21)*. The excitation wavelength

was selected by a double monochromator (Jobin Yvon UV-DH10, bandwidth 4 nm). A MCP-PMT Hamamatsu (model R3809U-02) was used. Time resolution was ~20 ps and the data were stored in 2048 channels. Automatic sampling cycles including 30 s accumulation time for the instrumental response function and 90 s acquisition time for each polarized component were carried out such that a total number of 2−4 $\times 10^6$ counts was reached in the fluorescence intensity decay.

Analysis of the Time-Resolved Fluorescence Data. Analyses of fluorescence intensity and anisotropy decays as sums of exponentials were performed by the maximum entropy method *(22−24)*. Details of the principles and application of the method to fluorescence decays have been previously published *(26−32)*.

Circular Dichroism Measurements. CD spectra were measured with a F-710 spectropolarimeter (Jasco, Japan) at room temperature (22 °C). The bandwidth was 2 nm, and the spectra were averaged over 10 scans of 100 nm per minute with integration time of 0.5 s. The spectra for the far-UV and near-UV regions were measured in 0.1 and 1 cm optical path cuvettes, respectively. Protein concentrations were ~2 and ~10 μM, respectively for the far- and the near-UV spectra.

RESULTS

1. The Effect of pH on the Steady-State Fluorescence Emission Spectrum of Trp187. The steady-state fluorescence spectrum of Trp187 in annexin V at neutral pH has a maximum at 326 nm. This testifies for a solvent inaccessible location, in agreement with the crystal structure of the protein without the calcium ion in domain III *(4)* (Figure 1A). In the presence of high calcium concentration (0.1M), the maximum of fluorescence emission is shifted to 350 nm *(9, 10, 12)*, demonstrating that the indole ring becomes exposed to the solvent, in agreement with the X-ray structure of the molecule with the calcium ion in its domain III *(5−7)* (Figure 1B).

The pH titration from the neutral region down to pH 3.5 in the absence of calcium shows a large progressive red-shift of the emission maximum of 12 nm, from 326 to 338 nm. This spectral shift is, however, smaller than that observed at the highest concentration of calcium *(9)*. The shift starts to occur at pH 6 and ends at pH ~4.5 with a midpoint situated around pH 5 (Figure 2). This pH range indicates that carboxylic side chains are probably involved. The width of the pH range in which the spectral change takes place suggests that more than one titratable acidic group may be involved in the process with p*K* around 4.6 and 5.6. No precipitation occurs when the protein is diluted in the proper acidic buffer at ~10 μM concentration as shown by the absorption spectrum (not shown), but direct titration inside the cuvette by progressive addition of small aliquots of 0.1N HCl led to partial precipitation of the protein.

In the alkaline pH region, a red-shift starts to appear as well (Figure 2). In this pH range, however, other phenomena can be involved, such as the formation of tyrosinate. We therefore did not titrate to pH higher than 11.

To test whether the effects of calcium and pH were associated, we measured the calcium-induced spectral shift at pH 7 and pH 5 in the millimolar concentration range. The results show, first, that the titration midpoint occurs at a concentration of calcium smaller at pH 5 than at pH 7 (respectively, 2 and 5 mM) and second, that the maximum spectral shift induced by calcium is significantely smaller at pH 5 (336 nm) than at pH 7 (340 nm) (Figure 3). This indicates that very weak calcium binding sites, which have been observed in the crystal structure to involve acidic side chains *(33)*, likely provoking larger spectral displacements at neutral pH, are suppressed at pH 5.

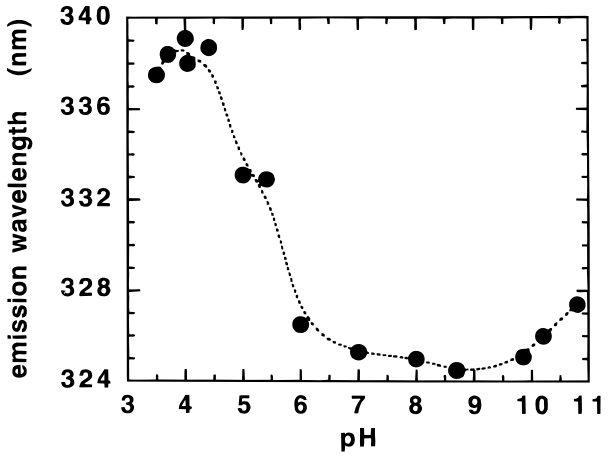

FIGURE 2: Variation of the maximum emission wavelength of Trp187 as a function of pH. Excitation wavelength: 295 nm (bandwidth 4 nm). Temperature: 20 °C.

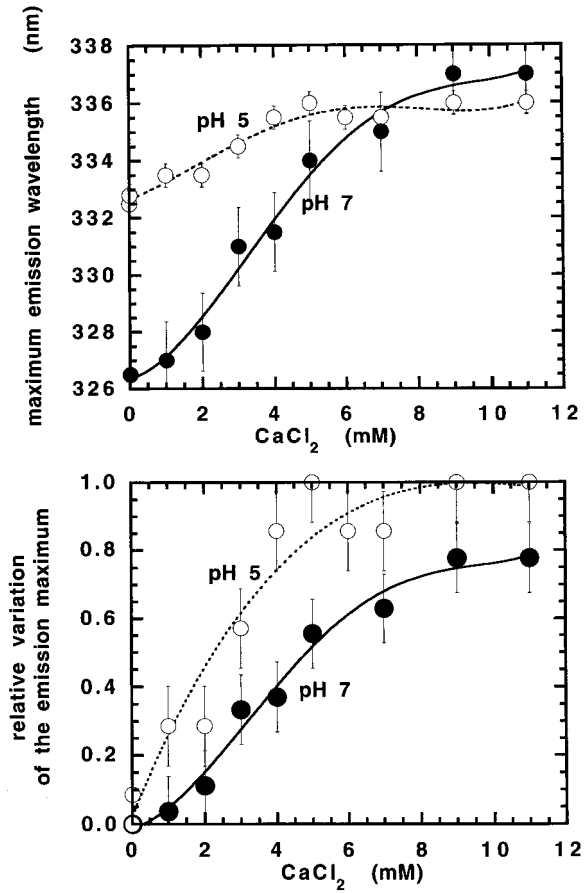

FIGURE 3: Variation of the maximum emission wavelength of Trp187 (upper figure) and of its relative proportion (lower figure) as a function of calcium chloride concentration. Experimental conditions: acetate buffer pH 5 and Tris-Cl buffer pH 5. Protein concentration: 10 μM.

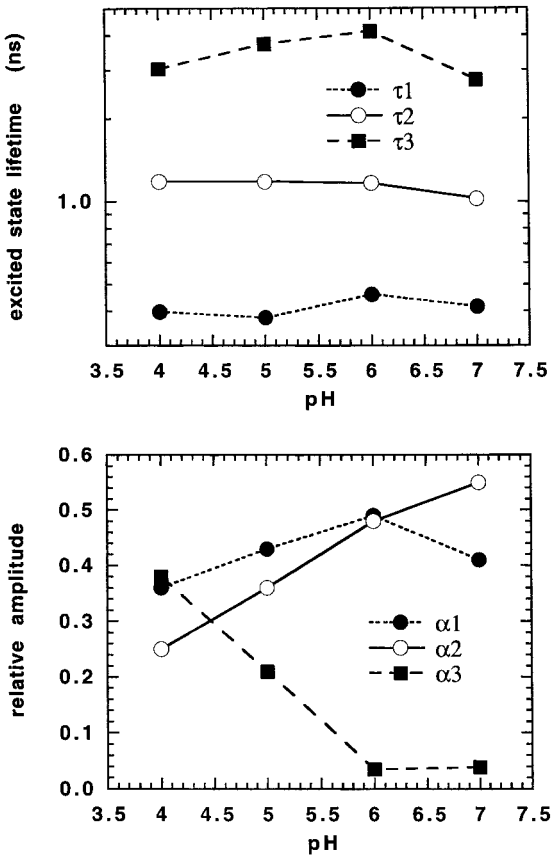

FIGURE 4: Variation of the excited-state lifetime values (upper figure) and of their relative proportions (lower figure) as a function of pH.

2. Excited-State Lifetime Heterogeneity of Trp187 as a Function of pH. Three excited-state lifetimes are necessary to describe the time-resolved fluorescence decay of the Trp187 residue at neutral pH, with a major lifetime population of 0.9−1 ns which represents 60% of the excited-state populations *(9, 11)*. This major lifetime corresponds most likely to the major indole conformer where the $N_{\epsilon 1}$ of the indole ring is H-bonded to the carbonyl group of the Thr224 main chain *(4)*. The electron acceptor properties of this group when it is involved in a peptide bond explain the quenching effect leading to the short excited-state lifetime for this conformer *(33, 34)*.

Lowering the pH leads to changes of the excited state lifetime distribution, mainly as far as the relative proportions are concerned, as shown in the spectrum resulting from MEM analysis of the data (Figure 4). The longest excited state lifetime increases in value and in proportion (Figure 5). At pH 3.8 it dominates the fluorescence emission and corresponds to 72% of the fluorescence intensity (Table 1), whereas at pH 7 it represents only 16% of the fluorescence intensity. This long lifetime is responsible for the red-shift of the steady-state emission spectrum. On the contrary, the proportion of the major lifetime of 0.9 ns at pH 7 decreases strongly (Figure 5). It is responsible for 75% of the relative fluorescence intensity at pH 7 and for only 28% at pH 3.8 (Table 1). This change of excited-state lifetime distribution parallels, but is not identical to, the one observed with calcium at high concentration *(9)* (Table 1).

3. The Accessibility of Trp187 to Water Soluble Quencher Acrylamide. To estimate the surface of the indole accessible

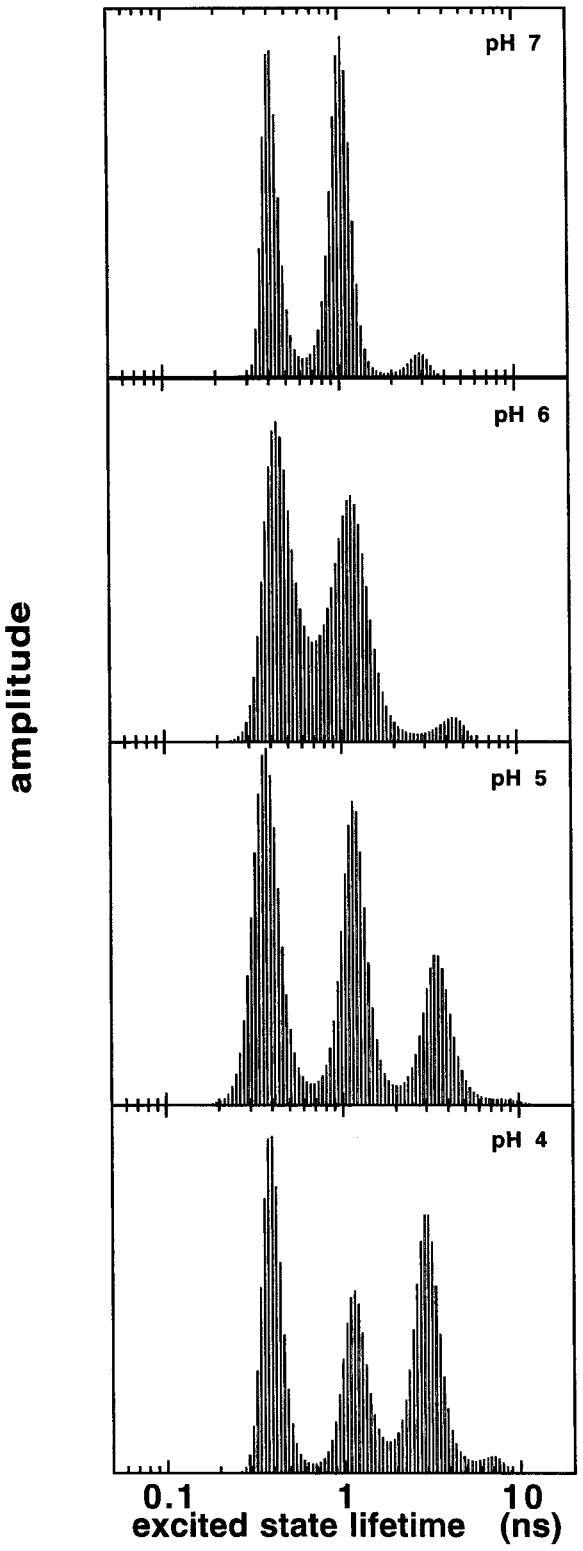

FIGURE 5: MEM reconstructed excited-state lifetime spectra of Trp187 fluorescence emission as a function of pH. Protein concentration: 10 μM. Cacodylate buffer at pH 7 and acetate buffer pH 6, 5, and 4. Excitation wavelength: 295 nm (bandwidth 4 nm). Emission wavelength: 335 nm (bandwidth 8 nm).

to the solvent, quenching experiments were performed by measuring the fluorescence decay as a function of acrylamide concentration for the protein at pH 7.5 in the absence of calcium, in the presence of 0.02 M calcium, and at pH 4. The Stern−Volmer plots of the ratios of the mean excited-state lifetime values without quencher and in the presence

Table 1: Fluorescence Decay Parameters of Trp187 in Annexin V as a Function of pH[a]

pH	τ_1 (ns) (C_1) (I_1)	τ_2 (ns) (C_2) (I_2)	τ_3 (ns) (C_3) (I_3)	$<\tau>$ (ns)
7	3.04	0.97	0.32	0.90
	(0.04)	(0.72)	(0.24)	
	(0.16)	*(0.75)*	*(0.08)*	
3.8	3.26	1.39	0.46	1.86
	(0.41)	(0.27)	(0.32)	
	(0.72)	*(0.28)*	*(0.08)*	
7 + calcium 0.01 M	3.57	1.18	0.46	2.23
	(0.45)	(0.40)	(0.15)	
	(0.72)	*(0.21)*	*(0.07)*	
7 + calcium 0.09 M	3.82	1.21	0.42	1.44
	(0.20)	(0.43)	(0.37)	
	(0.53)	*(0.36)*	*(0.11)*	

[a] Protein concentration: 10 μM. Temperature: 20 °C. Excitation wavelength: 295 nm (bandwidth 4 nm). Emission wavelength: 335 nm at pH 3.8−7, and 350 nm at pH 7 in the presence of calcium (bandwidth: 8 nm). The mean lifetime $<\tau>$ was calculated as $<\tau> = \sum_i C_i\tau_i$. C_i are the relative surface area of the lifetime peaks, and I_i are the relative associated intensities of each lifetime population $I_i = C_i\tau_i/\sum_i C_i\tau_i$.

Table 2: Acrylamide Quenching Constants Obtained by the Stern−Volmer Representation of the Mean Excited-State Lifetime Ratio $<\tau_0>/<\tau>$ as a Function of Acrylamide Concentration, for Annexin V in Tris-HCl Buffer pH 7.5, in the Absence and in the Presence of 0.02 M Calcium, and in Acetate Buffer pH 4 in the Absence of Calcium[a]

sample	K_{sv} (M^{-1})	$<\tau>$ (ns)	k_q (M^{-1} s^{-1})
pH 7.5	0.39	0.97	4.02×10^8
pH 7.5 + $CaCl_2$ 0.02 M	3.51	2.09	1.68×10^9
pH 4	2.44	1.74	1.40×10^9

[a] Protein concentration: 10 μM.

of increasing concentration of acrylamide are linear in the three cases. The Stern−Volmer and bimolecular quenching constant values are listed in Table 2. The bimolecular quenching constant value for Trp187 in annexin V at neutral pH in the absence of calcium is low as compared to that for solvent accessible Trp residues such as *N*-acetyltryptophan amide in water ($6-7 \times 10^9$ M^{-1} s^{-1}), small water-soluble peptides such as melittin, ACTH, or glucagon, but it is comparable to that of proteins with buried Trp residues such as RNAse T1 and the B subunit of cholera toxin *(for a review, see ref 35)*. The Trp187 of annexin V at neutral pH is therefore weakly accessible to acrylamide. According to Johnson and Yguerabide *(36)*, a surface area accessible to the quencher of ∼5% can be estimated. At pH 4, in contrast, the bimolecular quenching constant value increases strongly by a factor of ∼4, which indicates an accessibility of about 60%. In the presence of high calcium concentration at neutral pH, the accessibility of the Trp187 is also high, of the order of 80%. These results are in complete agreement with the red-shift of the maximum of fluorescence emission observed by decreasing the pH. The Trp187 residue becomes more solvent exposed in the conformation of domain III in mild acidic conditions.

4. The Local Dynamics of Domain III in Annexin V as a Function of pH: Subnanosecond Rotational Motion of the Indole Ring of Trp187 and Excited-State Lifetime Heterogeneity. The pattern of the impulse fluorescence anisotropy decay trace at pH 7 shows first a fast decrease followed by a transient rise and ends by a decrease which should go to zero since the overall Brownian rotation is isotropic (Figure 6). The complete trace of the anisotropy decay is not shown on the figure because the signal/noise ratio at long times is very low, owing to the short mean excited-state lifetime of 0.8 ns, compared to the value of the rotational correlation time of the protein (∼14 ns). Such a peculiar pattern for the impulse anisotropy decay was found in the case of the single Trp-containing protein FKBP12, where it corresponds to a strong coupling between the major short-lived excited state with a fast internal motion *(37)*. This suggests a similar specific coupling in annexin V between the short-lived emittor and the fastest rotation on one hand, and of the long-lived emittor with the long rotation (Brownian motion of the protein) on the other.

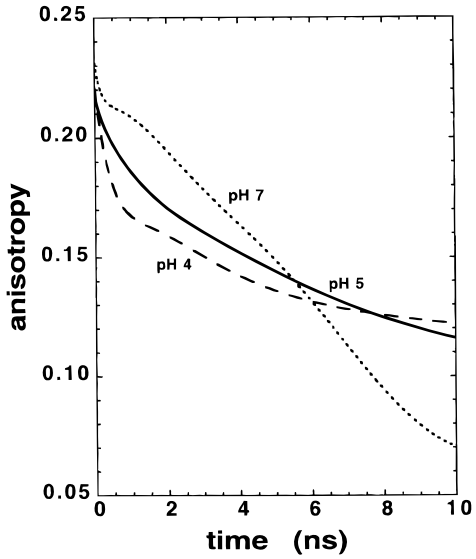

FIGURE 6: Impulse fluorescence anisotropy decay of Trp187 as a function of pH. Experimental conditions as in Figure 4.

Table 3: Fluorescence Anisotropy Decay Parameters of Trp187 in Annexin V as a Function of pH[a]

pH	A_S	θ_1 (ns)	θ_2 (ns)	β_1	β_2
7	0.221 ± 0.003	14.7 ± 0.4		0.224 ± 0.008	
6	0.214	15.3		0.221	
5	0.198	13.2	∞	0.133	0.057
4	0.170	5.1	∞	0.069	0.112

[a] Analysis by the correlated model as a sum of exponentials $A_t = \sum_i \beta_i \exp(-t/\theta_i)$. Protein concentration: 10 μM. Temperature: 20 °C. Excitation wavelength: 295 nm (bandwidth 4 nm). Emission wavelength: 335 nm (bandwidth: 8 nm). The standard error shown for the values at pH 7 is similar for the other measurements. A_s is the steady-state anisotropy.

The fluorescence polarized decay data were first analyzed by the one-dimensional model of the anisotropy which correlates all the lifetimes with all the rotational correlation times. These analyses did not detect any fast rotational motion of the indole ring at pH 7 (Table 3) *(9)*. Only the presence of the rotational correlation time of the monomeric protein is revealed. This was also observed for the FKBP12 protein as previously quoted *(38)* and in simulation experiments (ref *24*; and Vincent, unpublished data). The existence of a specific coupling between lifetime and correlation time can be revealed by the two-dimensional analysis of the polarized fluorescence decays *(24, 27, 37)*. The result of the analysis is represented as two-dimensional contour plots

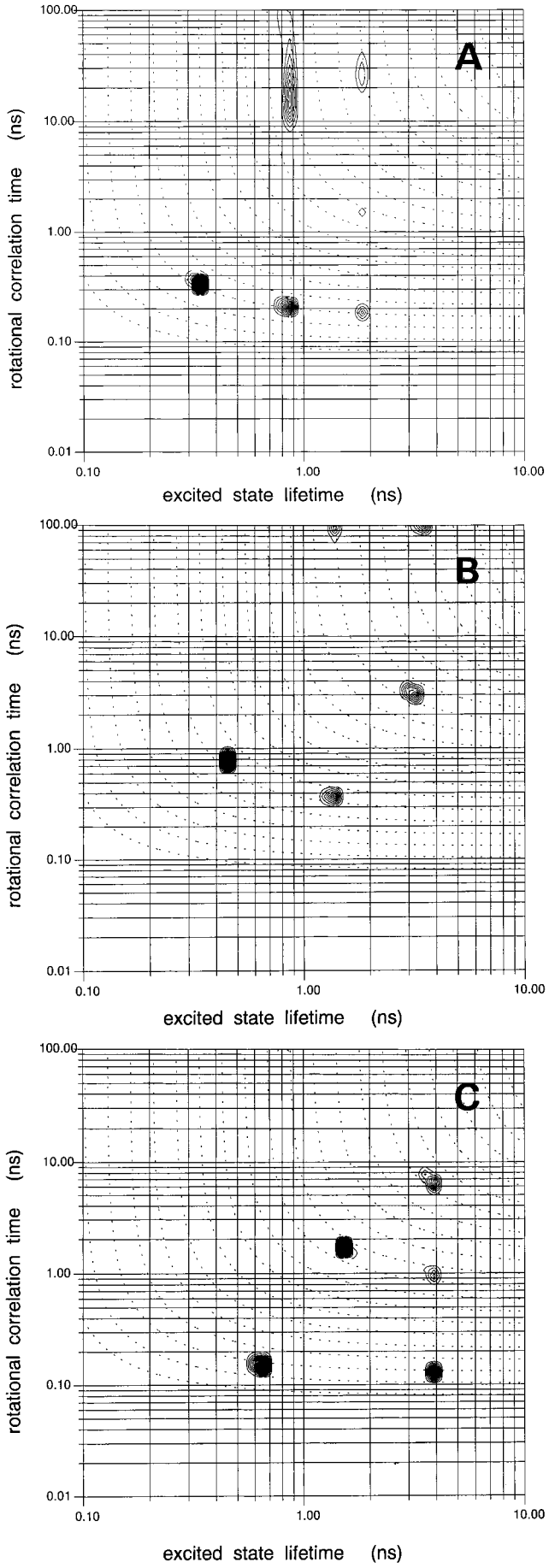

FIGURE 7: MEM reconstructed $\Gamma(\tau, \theta)$ plots at pH 7 (A), at pH 4 (B), and at 0.09 M calcium at pH 7 (C).

Table 4: Distribution of the $\Gamma(\tau,\theta)$ Obtained by Two-Dimensional Analysis of the Polarized Fluorescence Decays at Two Different pHs

pH 7			
θ (ns)	$\tau = 0.34$ ns	$\tau = 0.86$ ns	$\tau = 1.85$ ns
0.3	0.25	0.16	0.05
2	0	0	0.02
15	0	0.41	0.08
∞	0	0	0
pH 4			
θ (ns)	$\tau = 0.46$ ns	$\tau = 1.39$ ns	$\tau = 3.26$ ns
0.6	0.38	0.14	0
3	0	0	0.23
15	0	0	0
∞	0	0.11	0.14

(Figure 7). The results are presented in Table 4, where we have summarized the values of the $\Gamma(\tau, \theta)$ coefficients, which represent the relative proportion of a given population of chromophore with lifetime τ and rotational correlation time θ in the expressions of the polarized decays:

$$l_{vv}(t) = \int_0^\infty \int_0^\infty \Gamma(\tau, \theta)\, e^{-t/\tau} (1 + 2Ae^{-t/\theta})\, d\tau\, d\theta$$

$$l_{vh}(t) = \int_0^\infty \int_0^\infty \Gamma(\tau, \theta)\, e^{-t/\tau} (1 - Ae^{-t/\theta})\, d\tau\, d\theta$$

The shortest-lived excited state appears to be associated only with a fast rotational motion (200−300 ps) probably describing the rotational motion of the indole ring within its hydrophobic pocket. The major excited state of 0.9 ns is associated both with the long (∼15 ns) and with the short rotational correlation time of the protein (Figure 7A).

The impulse fluorescence anisotropy decays are quite different at acidic pH. At pH 5, the fast initial decay is more pronounced than at pH 7 (Figure 6). It is followed by a slower decrease than at neutral pH. The one-dimensional model analysis of the polarized fluorescence decays is able to detect the Brownian rotational correlation time of the protein. It reveals also the existence of an infinite anisotropy value (Table 3). This plateau value of the anisotropy suggests the presence of protein aggregates of large size. The rotational correlation time of the aggregate should be larger than about 10 times the longest excited-state lifetime (θ > 40 ns) (Table 1), a value which is intermediate between a dimer and a trimer. At this pH, the ratio of the infinite anisotropy value over the initial anisotropy indicates that about 30% of the protein is aggregated, the majority of the protein molecules being still monomeric.

At pH 4, the impulse fluorescence anisotropy decay shows that the initial decrease of the anisotropy is steeper than at the two other pHs. It is followed by a slight rising part and a slow decrease which never tends to zero, but reaches a plateau at around an infinite anisotropy value of 0.11 (Figure 6). The analysis by the one-dimensional model of the anisotropy shows the existence of a hindered rotational motion described by a 2 ns rotational correlation time and a high plateau value of the anisotropy at long times but no evidence for the correlation time of the monomeric form (Table 3). The protein is probably totally in the aggregated form(s). The two-dimensional analyses are not in contradiction with the former ones as far as the existence of the infinite

value of the anisotropy at pH 5 and 4 is concerned. They reveal, however, specific connectivities between lifetimes and correlation times. At pH 4, the analysis shows also the existence of a coupling between the short excited-state lifetime and the fastest rotational motion (Figure 7B). The two long lifetimes are associated with infinite correlation time values. This shows that as at pH 7, these two excited-state populations correspond to hindered conformers, whereas the short lifetime corresponds to a conformer in which the indole ring rotates freely but with a much slower rate than at pH 7.

The local dynamics of Trp187 in the high-calcium form of the protein 0.095 M $CaCl_2$ is however quite different as compared to that at pH 4. Three excited-state lifetime populations are present as in the other forms of the protein *(10)*. The shortest-lived excited state corresponds to a rapidly moving conformer as in the other forms also, but as compared to the low pH conformation, the rotational dynamics of the indole ring is faster (100−200 ps) than that of the calcium-free form at neutral pH (300 ps) and even more so than the acidic form of the protein (600−900 ps) (Figure 7C). By contrast, the lifetime population of 1 ns appears to correspond to faster rotations in the acidic form than in the high-calcium form. In the former case, however, this rotation is limited (presence of infinite values affecting this lifetime population). The longest lifetime corresponds to a highly mobile conformer in the high-calcium form but not in the acidic form.

The indole ring is therefore more exposed to the solvent in the high-calcium form than in the acidic form of the protein. At the same time, in the high-calcium form it displays faster rotations and almost no rotational hindrances. No aggregates are observed.

5. Examination of the Change in the Microenvironment of the Trp187 Residue and of the Secondary Structure of Annexin V by Circular Dichroism as a Function of pH. The overall secondary structure of the protein is not significantly modified upon decreasing the pH from 7 to 4 (Figure 8A). The dichroic bands characteristic of an α-helical structure are even reinforced at acidic pH as compared to neutral pH. On the other hand, the dichroic bands in the near-UV region, which is related to the environment of the aromatic amino acids and more particularly to the Trp residue, follow a similar variation as a function of pH (Figure 8B) as with increasing calcium concentration *(9)*.

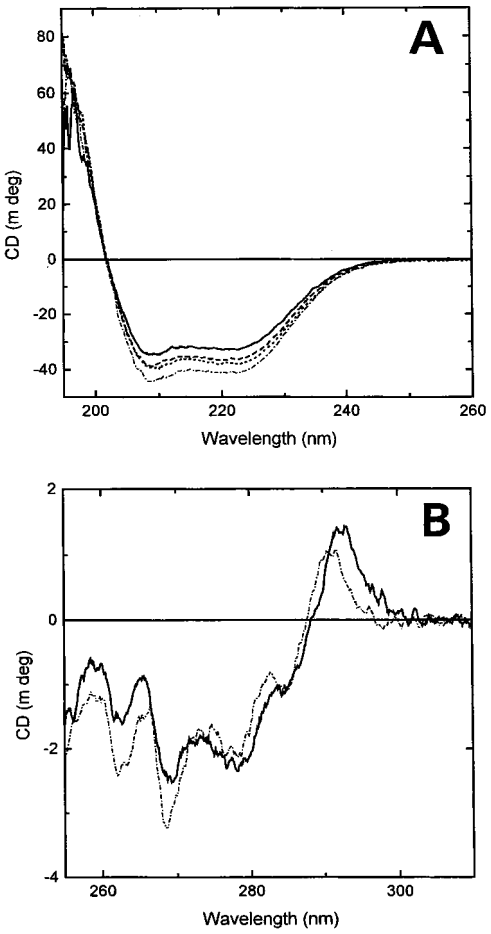

FIGURE 8: Circular dichroism spectra of annexin V as a function of pH. (A) far-UV spectra: from top to bottom pH 7, pH 6, pH 5, and pH 4; (B) near-UV spectra: plain line pH 7, dotted line pH 4.

DISCUSSION

The existence of a conformational adaptability of domain III of annexin V has been suggested by different physical techniques, especially fluorescence, under different conditions. In particular, a conformational change has been detected in this domain as a function of calcium concentration *(9, 12)* and also after interaction with negatively charged phospholipid membranes *(8, 11, 13)*. During this conformational change, the Trp187 residue is moved from a buried location between helices IIIA and IIIB to the protein surface in contact with the solvent *(5−7)*. The molecular mechanism that triggers the conformational change induced in these different situations, and especially the need for a high calcium concentration, is however still not well understood since, in the absence of the divalent ion, no calcium binding site is available in domain III.

The conformational flexibility of domain III is supported by the observation of multiexponential fluorescence decays of Trp187 which shows three excited-state lifetime populations *(10, 12)*. This heterogeneity of fluorescence emission suggests that different local conformations coexist, according to the conformer model that has been proposed to explain the multiexponential decays of Trp and its derivatives in solution as well as in short peptides *(31, 38−44)*. Dynamic quenching interactions with protein moieties (peptide bonds or protonated amino acid side chains, disulfide bridges) may occur with different efficiencies in the respective conformers *(33, 34, 45−53)*. The quenching efficiency depends not only on the distance between the chromophore and the quenching groups but also on the local subnanosecond dynamics.

The two-dimensional analysis of the polarized fluorescence decays in terms of connectivities between lifetimes (τ) and correlation times (θ) indicates that the excited state heterogeneity of Trp187 in annexin V is associated with a rotational heterogeneity. This lends further support to the existence of "conformational substates" where the Trp187 residue displays different mobilities. The shortest excited-state lifetime is connected only with a fast subnanosecond rotational motion, whereas the major lifetime is associated with this fast motion but also with the overall Brownian rotational motion of the protein. The fast rotational motion of Trp187 is therefore submitted to different rotational constraints in the respective conformers. This suggests the existence of slow "breathing motions" of the structural

elements in the proximity of the Trp187 residue. Such "respiratory" motions are also suggested by modelization of the conformational transition of domain III induced by calcium (Sopkova et al., in preparation). Therefore, we can assume that the potentiality for conformational adaptability exists in this region of the protein. pH should affect polar interactions involved in the stabilization of the local folding of the protein and can lead to the observed conformational change.

The examination of the different crystal structures of annexin V with and without calcium bound in domain III, may provide further indications of the electrostatic interactions involved in the stabilization of the conformation of the protein in its different forms which could explain the pH effect. Several crystal structures have been published using different crystallization conditions. We have focused our observations only on the structures presenting the highest available resolution, namely the R3 structure without calcium in domain III (resolution 2.0 Å) *(32)* and the P1 structure containing the calcium ion in domain III (resolution: 1.9 Å) *(5)*. These two crystal forms can be obtained under the same crystallization conditions and can coexist in the same drop *(5)*.

Several salt bridges and H-bonds are affected in domain III by calcium binding to this domain. In particular, the H-bond between $O_{\gamma 1}$ of Thr229 and $O_{\gamma 1}$ of Asp226 disappears when calcium is bound in domain III. A $-120°$ rotation of the ψ angle of Asp226 was also observed in the calculations mentioned above (Sopkova et al., in preparation). By contrast, a salt bridge is formed between $O_{\epsilon 1}$ from Glu184 and $N_{\epsilon 1}$ from Arg227 when calcium is bound (distance 3.11 Å). We can remark that in annexin III, where the Trp residue in domain III (Trp191) is exposed to the solvent in the absence of calcium at neutral pH *(55)*, Asp226 is replaced by a Lys residue. Therefore, the H-bond interaction with Thr229 is suppressed in this protein.

Another salt bridge is present in the R3 structure between $N_{\zeta 1}$ of Lys193 and $O_{\gamma 1}$ of Asp190 (distance: 2.52 Å) and stabilizes the loop between helices IIIA and IIIB. This salt bridge is weaker in the form with the calcium ion bound in domain III (distance: 3.47 Å). Calculations performed recently with the conjugated peak refinement method in order to model the reaction pathway of the conformational change of domain III elicited by calcium, suggest that the geometry of the peptide bond involving Asp190 may undergo a trans-cis-trans transition during the conformational change. Moreover, this residue undergoes a $-120°$ rotation about the φ angle during the transition (Sopkova et al., in preparation).

The balance of few specific electrostatic interactions seems therefore to be quite important in the stabilization of domain III and in the pathway that ends up in opening the calcium binding site in this domain. These interactions may be weakened in mild acidic pH conditions in such a way that the calcium binding site becomes more open and more accessible to the calcium ion than at neutral pH. Nevertheless, charged side chains situated in other parts of the protein can also be involved in this process. In this respect, it has recently been shown that a partial truncation of the N-terminal region of the protein (removal of the first 9 residues, in particular Arg5) led to partial exposure of Trp187 to the solvent, corresponding to a small red-shift of the fluorescence emission spectrum by 4−5 nm *(55)*. Moreover, the exposed conformation of the Trp187 residue has been observed in the crystal structure of another mutant of annexin V, where the Glu95 residue situated in the central channel has been replaced by Ser *(7)*.

Finally, in parallel with the conformational change, the anisotropy data show that an aggregation process takes place. It could be related to an increased hydrophobicity of the protein at acidic pH which may facilitate its auto-association via non-repulsive interactions involving uncharged surface regions *(19)*.

In conclusion, these observations suggest that the conformational change of domain III does not absolutely require calcium binding but can be provoked by a pH change. This may give some clues to the mechanism of the conformational change of domain III elicited upon binding of the protein to negatively charged phospholipid membranes. Changes of the apparent p*K*s of the acidic ionizable groups in the membrane hydration layer are likely to occur, due to the increase of the proton activity *(56−59)*. This may facilitate the conformational change of the protein on the membrane surface, without the need for a high calcium concentration.

ACKNOWLEDGMENT

We are very grateful to Dr. I. Maurer-Fogy (Bender and Co., Vienna, Austria) for a generous gift of pure recombinant human annexin V. The technical staff of L.U.R.E. is acknowledged for running the synchrotron ring during the beam sessions.

REFERENCES

1. Gerke, V., and Moss, S. E. (1997) *Biochim. Biophys. Acta 1357,* 129−154.
2. Raynal, P., and Pollard, H. B. (1994) *Biochim. Biophys. Acta 1197,* 63−93.
3. Swairjo, M. A., and Seaton, B. A. (1994) *Annu. Rev. Biophys. Biomol. Struct. 23,* 193−213.
4. Huber, R., Berendes, R., Burger, A., Schneider, M., Karshikov, A., Luecke, H., Romisch, J., and Paques, E. P. (1992) *J. Mol. Biol. 223,* 683−704.
5. Sopkova, J., Renouard, M., and Lewit-Bentley A. (1993) *J. Mol. Biol. 234,* 816−825.
6. Concha, N. O., Head, J. F., Kaetzel, M. A., Dedman, J. R., and Seaton, B. A. (1993) *Science 261,* 1321−1324.
7. Berendes, R., Voges, D., Demange, P., Huber, R., and Burger, A. (1993) *Science 262,* 427−430.
8. Meers, P. (1990) *Biochemistry 29,* 3325−3330.
9. Sopkova, J., Gallay, J., Vincent, M., Pancoska, P., and Lewit-Bentley, A. (1994) *Biochemistry 33,* 4490−4499.
10. Pigault, C., Follenius-Wund, A., Schmutz, M., Freyssinet, J.-M., and Brisson, A. (1994) *J. Mol. Biol. 236,* 199−208.
11. Follenius-Wund, A., Piémont, E., Freyssinet, J.-M., Gérard, D., and Pigault, C. (1997) *Biochem. Biophys. Res. Commun. 234,* 111−116.
12. Meers, P., and Mealy, T. R. (1993) *Biochemistry 32,* 5411−5418.
13. Sopkova, J. (1994) Ph.D. Thesis, Universities of Prague and Orsay.
14. Meers, P. (1996) in *Annexins: Molecular Structure to Cellular Function* (Seaton, B. A., Ed.) R. G. Landes Company, Austin, TX.
15. Onishi, S., and Hito, T. (1973) *Biochim. Biophys. Res. Commun. 51,* 132−138.
16. Onishi, S., and Hito, T. (1974) *Biochemistry 13,* 881−887.
17. Hito, T., and Onishi, S. (1974) *Biochim. Biophys. Acta 352,* 509−529.

18. Van Dijck, P. W. M., De Kruijff, B., Verkleij, A. J., Van Deenen, L. L. M., and De Gier, J. (1978) *Biochim. Biophys. Acta 512*, 84−96.
19. Köhler, G., Hering, U., Zschörnig, O., and Arnold, K. (1997) *Biochemistry 36*, 8189−8194.
20. Maurer-Fogy, I., Reutelingsperger, C. P. M., Peiters, J., Bodo, G., Stratowa, C., and Hauptman, R. (1988) *Eur. J. Biochem. 174*, 585−592.
21. Vincent, M., Gallay, J., and Demchenko, A. P. (1995) *J. Phys. Chem. 99*, 14931−14941.
22. Livesey, A. K., Licinio, P., and Delaye, M. (1986) *J. Chem. Phys. 84*, 5102−5107.
23. Livesey, A. K., and Brochon, J. C. (1987) *Biophys. J. 52*, 693−706.
24. Brochon, J.-C. (1994) *Methods Enzymol. 240*, 262−311.
25. Vincent, M., Brochon, J.-C., Mérola, F., Jordi, W., and Gallay, J. (1988) *Biochemistry 27*, 8752−8761.
26. Mérola, F., Rigler, R., Holmgren, A., and Brochon, J.-C. (1989) *Biochemistry 28*, 3393−3398.
27. Gentin, M., Vincent, M., Brochon, J. C., Livesey, A. K., Cittanova, N., and Gallay, J. (1990) *Biochemistry 29*, 10405−10412.
28. Kuipers, O. P., Vincent, M., Brochon, J.-C., Verheij, H. M., de Haas, G. H., and Gallay, J. (1991) *Biochemistry 30*, 8771−8785.
29. Vincent, M., Li de la Sierra, I. M., Berberan-Santos, M. N., Diaz, A., Diaz, M., Padron, G., and Gallay, J. (1992) *Eur. J. Biochem. 210*, 953−961.
30. Gallay, J., Vincent, M., Li de la Sierra, I. M., Alvarez, J., Ubieta, R., Madrazo, J., and Padrón, G. (1993) *Eur. J. Biochem. 211*, 213−219.
31. Bouhss, A., Vincent, M., Munier, H., Gilles, A.-M., Takahashi, M., Bârzu, O., Danchin, A., and Gallay, J. (1996) *Eur. J. Biochem. 237*, 619−628.
32. Lewit-Bentley, A., Bentley, G. A., Favier, B., L'Hermite, G., and Renouard, M. (1994) *FEBS Lett. 345*, 38−42.
33. Steiner, R. F., and Kirby, E. P. (1969) *J. Phys. Chem. 73*, 4130−4135.
34. Chen, Y., Liu, B., Hong-Tao, Y., and Barkley, M. D. (1996) *J. Am. Chem. Soc. 118*, 9271−9278.
35. Eftink, M. (1991) in *Topics in Fluorescence Spectroscopy* (Lakowicz, J. R., Ed.) Principles, Vol. 2, Chapter 2, pp 53−126, Plenum Press, New York.
36. Johnson, D. A., and Yguerabide, J. (1985) *Biophys. J. 48*, 949−955.
37. Rouvière, N., Vincent, M., Craescu, C. T., and Gallay, J. (1997) *Biochemistry 36*, 7339−7352.
38. Donzel, B., Gauduchon, P., and Wahl, Ph. (1974) *J. Am. Chem. Soc. 96*, 5001−5007.
39. Szabo, A. G., and Rayner, D. M. (1980) *J. Am. Chem. Soc. 102*, 554−563.
40. Petrich, J. W., Chang, M. C., McDonald, D. M., and Fleming, G. R. (1983) *J. Am. Chem. Soc. 105*, 3824−3832.
41. Alcala, J. R., Gratton, E., and Prendergast, F. G. (1987) *Biophys. J. 51*, 925−936.
42. Philips, L. A., Webb, S. P., Martinez, S. J., III, Fleming, G. R., and Levy, D. H. (1988) *J. Am. Chem. Soc. 110*, 1352−1355.
43. Ross, J. B. A., Wyssbrod, H. R., Porter, R. A., Schwartz, G. P., Michaels, C. A., and Laws, W. R. (1992) *Biochemistry 31*, 1585−1594.
44. Willis, K. J., Neugebauer, W., Sikorska, M., and Szabo, A. G. (1994) *Biophys. J. 66*, 1623−1630.
45. Cowgill, R. W. (1962) *Biochim. Biophys. Acta 133*, 6−18.
46. Cowgill, R. W. (1967) *Biochim. Biophys. Acta 140*, 37−44.
47. Bushueva, T. L., Busel, E. P., Bushueva, V. N., and Burstein, E. A. (1974) *Stud. Biophys. 44*, 129−139.
48. Bushueva, T. L., Busel, E. P., and Burstein, E. A. (1975) *Stud. Biophys. 52*, 41−52.
49. Ricci, R. W., and Nesta, J. M. (1976) *J. Phys. Chem. 80*, 974−980.
50. Shizuka, H., Scrizawa, M., Shimo, T., Saito, I., and Matsuura, T. (1988) *J. Am. Chem. Soc. 110*, 1930−1934.
51. Tilstra, L., Sattler, M. C., Cherry, W. R., and Barkley, M. D. (1990) *J. Am. Chem. Soc. 112*, 554−563.
52. McMahon, L. P., Colucci, W. J., McLaughlin, M. L., and Barkley, M. D. (1992) *J. Am. Chem. Soc. 114*, 8442−8448.
53. Vos, R., and Engelborghs, Y. (1994) *Photochem. Photobiol. 60*, 24−32.
54. Favier-Perron, B., Lewit-Bentley, A., and Russo-Marie, F. (1996) *Biochemistry 35*, 1740−1744.
55. Arboledas, D., Olmo, N., Lizarbe, A., and Turnay, J. (1997) *FEBS Lett. 416*, 217−220.
56. Teissié, J., Prats, M., Soucaille, P., and Tocanne, J. F. (1985) *Proc. Natl. Acad. Sci. U.S.A. 82*, 3217−3221.
57. Tocanne, J. F., and Teissié, J. (1990) *Biochim. Biophys. Acta 1031*, 111−142.
58. Beschiaschvili, G., and Seelig, J. (1992) *Biochemistry 31*, 10044−10053.
59. Israelachvili, J., and Wennerström, H. (1996) *Nature 379*, 219−225.
60. Kraulis, P. J. (1991) *Appl. Crystallogr. 24*, 946−950.

BI980773O